

Long-range magnetic order and spin-lattice coupling in the delafossite CuFeO_2

Volker Eyert,* Raymond Frésard, and Antoine Maignan
Laboratoire CRISMAT, UMR CNRS-ENSICAEN(ISMRA) 6508,
6, Boulevard Maréchal Juin, 14050 Caen Cedex, France
(Dated: September 11, 2018)

The electronic and magnetic properties of the delafossite CuFeO_2 are investigated by means of electronic structure calculations. They are performed using density functional theory in the generalized gradient approximation as well as the new full-potential augmented spherical wave method. The calculations reveal three different spin states at the iron sites. Taking into account the correct crystal structure, we find long-range antiferromagnetic ordering in agreement with experiment. Contrasting previous work, our calculations show that non-local exchange interactions lead to a semiconducting ground state.

PACS numbers: 71.20.-b, 75.25.+z, 75.30.Et, 73.90.+f, 75.50.Pp

Keywords: electronic structure, low-dimensional compounds, magnetic semiconductors, exchange interactions, geometric frustration

Long-range magnetic ordering on triangular lattices with antiferromagnetic exchange interactions is at the focus of continuing interest. This is due to the strong geometric frustration experienced by such systems, which may lead to a large variety of magnetic states including incommensurate and non-collinear spin arrangements. As a consequence, there is usually a complex response to magnetic fields, which gives rise, e.g., to magnetization steps [1, 2, 3]. While this behavior has been observed in the trigonal chain cobaltates, where it leads to a striking spin dynamics [2], the genuine situation is that of well separated triangular layers as they are found, e.g., in the delafossite-type compounds ABO_2 .

In general, this broad class of materials has aroused much interest due to a broad range of exciting physical properties [4], including strongly anisotropic very high electrical conductivities as, e.g., in PdCoO_2 and semiconducting behavior in antiferromagnetic delafossites. High optical band gaps in Cu- and Ag-based materials allow for simultaneous transparency and p-type conductivity [5] and, hence, the development of transparent optoelectronic devices. This large variety is caused by the stacking of monoatomic triangular layers within the rhombohedral structure [4]. Edge-sharing distorted oxygen octahedra surrounding the B-atoms form BO_2 sandwich layers, which are linked to the A-atom layers via linear O–A–O bonds (for the crystal structure see also Fig. 1 of Ref. [6]). Generically, the A and B atoms are mono- and trivalent, respectively. Depending on the chemical composition, this opens a zoo of behaviors: for instance, if the A^+ ion is in a d^9 configuration good metallic conductivity is observed as in the case of PdCoO_2 , while if it is in a d^{10} configuration, the degrees of freedom dominating the low-energy physics are due to the B atoms as, e.g., in CuCrO_2 and AgCoO_2 .

As for many other magnetic delafossite compounds, the exact magnetic structure of CuFeO_2 has long been a matter of dispute [7, 8]. Using neutron diffraction, Mekata *et al.* were able to distinguish two different mag-

netic phases below $T_{\text{N}1} = 16$ K and $T_{\text{N}2} = 11$ K. They are connected with monoclinic and orthorhombic magnetic supercells, respectively, of the undistorted rhombohedral unit cell with commensurate and incommensurate collinear arrangements of the localized $4.4\mu_B$ Fe^{3+} moments [9, 10, 11, 12]. Observation of a noncollinear-incommensurate phase in magnetic field was taken as indicative of possible multiferroic behavior [12], which was indeed observed in Al-doped CuFeO_2 [13]. Quite recently, X-ray and neutron diffraction measurements by Ye *et al.* contrasted the previous observations by revealing structural distortions accompanying the magnetic phase transitions, which eventually lead to a monoclinic structure at 4 K [14].

Only few electronic structure calculations for magnetic delafossite compounds have been reported in the literature [15, 16, 17, 18]. From LDA calculations, Galakhov *et al.* obtained a ferromagnetic state for the rhombohedral $R\bar{3}m$ structure with a magnetic moment at the Fe site of about $0.9\mu_B$, much lower than the experimental value [15]. The Fe $3d$ t_{2g} states were found above the Cu $3d$ states just at E_{F} , in disagreement with both photoemission data and the fact that CuFeO_2 is a semiconductor with an optical band gap of about 1.15 eV. In contrast, LDA+U calculations led to a band gap of 2 eV and a magnetic moment of $3.76\mu_B$. However, the occupied Fe $3d$ states were located at about 9 eV below the valence band maximum and thus much too low [15]. Recent calculations by Ong *et al.* using the generalized gradient approximation (GGA) [20] resulted in a high-spin state with a magnetic moment of $3.78\mu_B$ per Fe and the Fe $3d$ t_{2g} spin-up states below the Cu $3d$ bands in agreement with photoemission and X-ray emission data [17]. However, again a finite optical band gap was arrived at only after taking into account electronic correlations within the LDA+U scheme [17].

In the present work we apply the new full-potential augmented spherical wave method to study the electronic properties of CuFeO_2 . In doing so, we take for the first

time the experimentally observed low-temperature structure into account. Our calculations resolve open issues by revealing i) an antiferromagnetic ground state for the monoclinic structure in perfect agreement with the experimental data, ii) the opening of a fundamental band gap already at the GGA level, i.e. without taking local correlations into account, and iii) the quite unusual existence of three different magnetic states of assumed ferromagnetic CuFeO_2 , which so far has been seen only for elemental iron [19].

The calculations are based on density-functional theory and the generalized gradient approximation (GGA) [20] with the local-density approximation parameterized according to Perdew and Wang [21]. They were performed using the scalar-relativistic implementation of the augmented spherical wave (ASW) method (see Refs. 22, 23, 24 and references therein). In the ASW method, the wave function is expanded in atom-centered augmented spherical waves, which are Hankel functions and numerical solutions of Schrödinger's equation, respectively, outside and inside the so-called augmentation spheres. In order to optimize the basis set, additional augmented spherical waves were placed at carefully selected interstitial sites. The choice of these sites as well as the augmentation radii were automatically determined using the sphere-geometry optimization algorithm [25]. Self-consistency was achieved by a highly efficient algorithm for convergence acceleration [26]. The Brillouin zone integrations were performed using the linear tetrahedron method with up to 1156 and 3180 \mathbf{k} -points within the irreducible wedge of the rhombohedral and monoclinic Brillouin zone, respectively [24, 27]. For the monoclinic magnetic supercell, up to 100 \mathbf{k} -points were used.

In the present work, a new full-potential version of the ASW method was employed [28]. In this version, the electron density and related quantities are given by spherical-harmonics expansions inside the muffin-tin spheres. In the remaining interstitial region, a representation in terms of atom-centered Hankel functions is used [29]. However, in contrast to previous related implementations, we here get away without needing a so-called multiple- κ basis set, which fact allows to investigate rather large systems with a minimal effort.

The calculations used the crystal structure data by Ye *et al.* [14]. As a starting point, spin-degenerate calculations for the rhombohedral structure were performed. The resulting partial densities of states (DOS) are shown in Fig. 1. While the lower part of the spectrum is dominated by O $2p$ states, the transition metal d states lead to rather sharp peaks in the interval from -3 to $+2$ eV. In particular, the t_{2g} and e_g manifolds of the Fe $3d$ states as resulting from the octahedral coordination are recognized. This representation of the partial DOS used a local rotated coordinate system with the Cartesian axes pointing towards the oxygen atoms. σ -type overlap of the O $2p$ states with the Fe $3d$ e_g orbitals leads to the

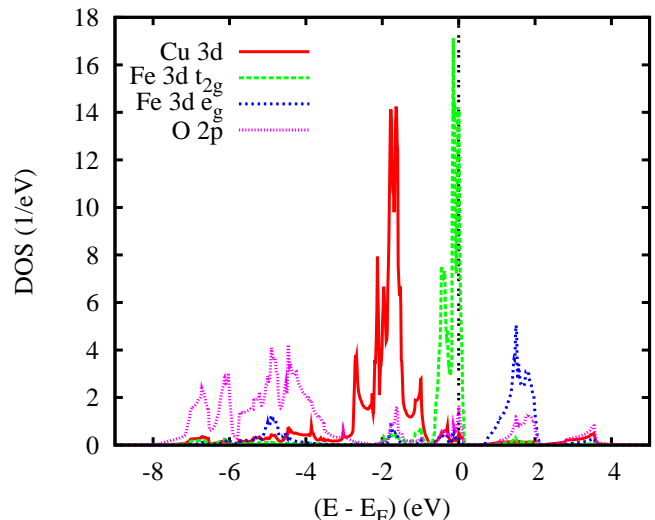


FIG. 1: (Color online) Partial densities of states (DOS) of rhombohedral CuFeO_2 . Selection of Fe $3d$ orbitals in this and the subsequent figures is relative to the local rotated reference frame, see text.

contribution of the latter near -5 eV. In contrast, due to the much weaker π -type overlap of the O $2p$ states with the t_{2g} orbitals, these states give rise to sharp peaks in the interval from -0.8 eV to just above the Fermi energy. The latter falls right into the upper part of the t_{2g} manifold and Fe turns out to be in a d^5 state. In contrast, the Cu $3d$ states are essentially limited to the interval from -3 to -1 eV and thus Cu can be assigned a monovalent d^{10} configuration in close analogy with the experimental findings. In passing, we mention the finite dispersion of the electronic bands parallel to Γ -A, which points to a considerable three-dimensionality arising from the coupling between the layers as has been observed also in other delafossite materials [6].

Since the perfect triangular lattice of the rhombohedral structure does not allow for long-range antiferromagnetic order, subsequent spin-polarized calculations were performed for an assumed ferromagnetic state in a spirit similar to the previous work by Galakhov *et al.* as well as by Ong *et al.* [15, 17]. From our calculations, three different configurations were obtained corresponding to a low-spin, intermediate-spin, and high-spin moment located at the Fe site. The respective partial densities of states are displayed in Fig. 2. The total energies as compared to the spin-degenerate configuration and the local magnetic moments are summarized in Tab. I. In general, the observation of three different spin states for magnetic ions is very unusual and so far has been reported only for elemental fcc Fe [19]. According to the partial DOS, the magnetic moments of the low-spin and intermediate-spin states are almost exclusively carried by the Fe $3d$ t_{2g} states, which show a spin splitting of about 1 and 2 eV, respectively. In the high-spin configuration this splitting

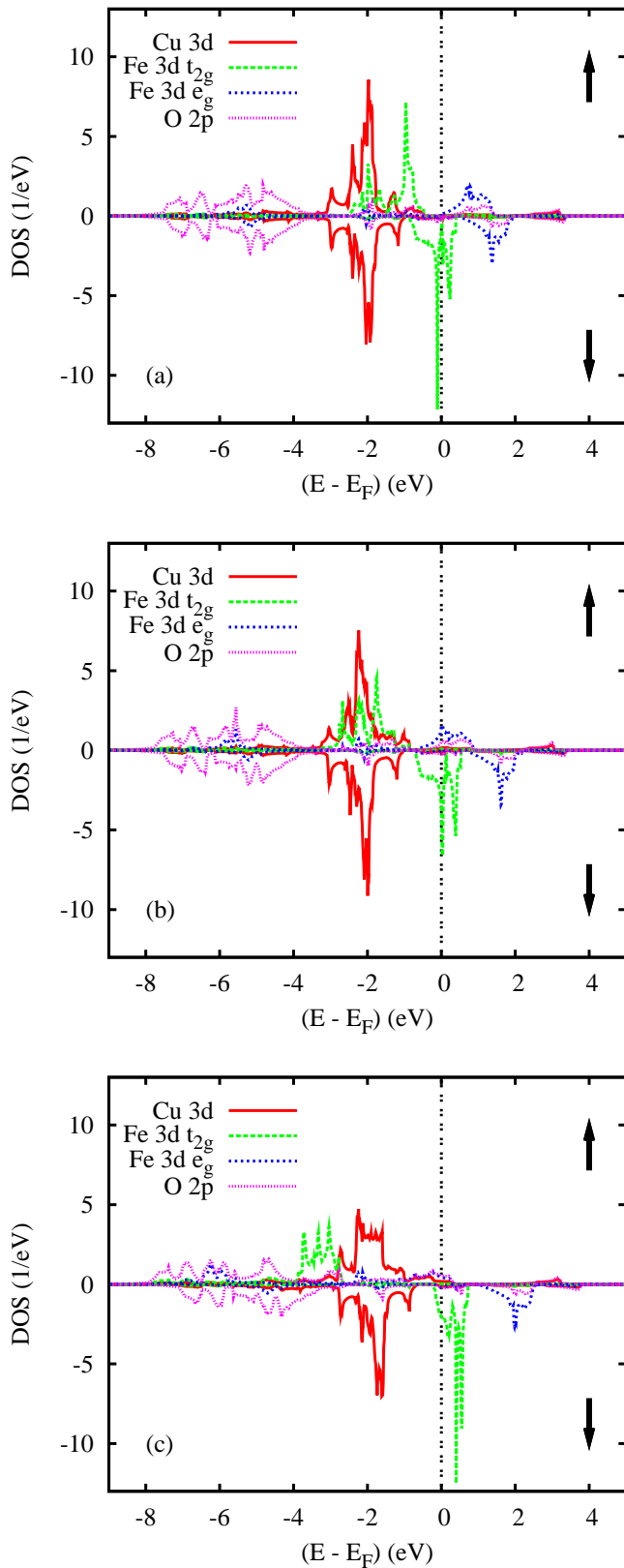


FIG. 2: (Color online) Partial densities of states (DOS) of rhombohedral ferromagnetic (a) low-spin, (b) intermediate-spin, and (c) high-spin CuFeO_2 .

TABLE I: Total energies (in mRyd per formula unit) and magnetic moments (in μ_B) for different crystal structures and magnetic orderings of CuFeO_2 .

structure	magn. order	ΔE	m_{Fe}	m_{O}
rhomb.	spin-deg.	0.0		
rhomb.	ferro (LS)	-16.7	1.03	-0.02
rhomb.	ferro (IS)	-12.0	2.02	-0.02
rhomb.	ferro (HS)	-19.2	3.73	0.21
monoclinic	spin-deg.	-6.0		
monoclinic	ferro (LS)	-21.5	1.04	-0.02
monoclinic	ferro (IS)	-19.0	2.08	-0.02
monoclinic	ferro (HS)	-32.0	3.62	0.19
monoclinic	antiferro	-46.0	± 3.72	± 0.08

increases to $\approx 3.5 \text{ eV}$ and the magnetic moment is carried by both the t_{2g} and e_g states. In addition, due to the strong σ -type overlap with the latter, the O $2p$ states also experience a substantial polarization. For the same reason, the e_g moments start to form already in the energy interval of the O $2p$ states leading to distinctly different spin-up and spin-down e_g partial DOS. A similar behavior has been also observed in other high-spin systems and termed as the formation of local extended magnetic moments [30]. As is obvious from Tab. I, all three ferromagnetic configurations have energies lower than the spin-degenerate situation. However, the high-spin state is most stable for the rhombohedral lattice. In summary, our calculations not only reproduce both the low-spin and high-spin results obtained by Galakhov *et al.* as well as by Ong *et al.* and explain the differences between their findings but additionally prove the existence of yet another, intermediate-spin state. Furthermore, the high-spin partial DOS compare very well with the photoemission and X-ray emission data [15].

In a second step, the monoclinic structure observed by Ye *et al.* was considered [14]. Note that in this structure there is still only one Fe atom per unit cell. Both the spin-degenerate and the spin-polarized ferromagnetic calculations led to essentially the same partial DOS as for the rhombohedral structure. In particular, again three different magnetic configurations were found with the local magnetic moments as listed in Tab. I being almost identical to those obtained for the rhombohedral structure. However, the total energies, also given in Tab. I, are generally lower by several mRyd with the largest energy lowering occurring for the high-spin state.

Finally, calculations for the eightfold magnetic supercell proposed by Ye *et al.* [14] were performed. The resulting partial DOS are displayed in Fig. 3 and the local magnetic moments and total energy included in Tab. I. According to these results, the antiferromagnetic state has the lowest energy as compared to all other configurations. In addition, Fe is found to be in a high-spin state in agreement with the neutron diffraction data by Mekata *et al.* [9, 10]. Remarkably, a band gap of 0.05 eV is obtained.

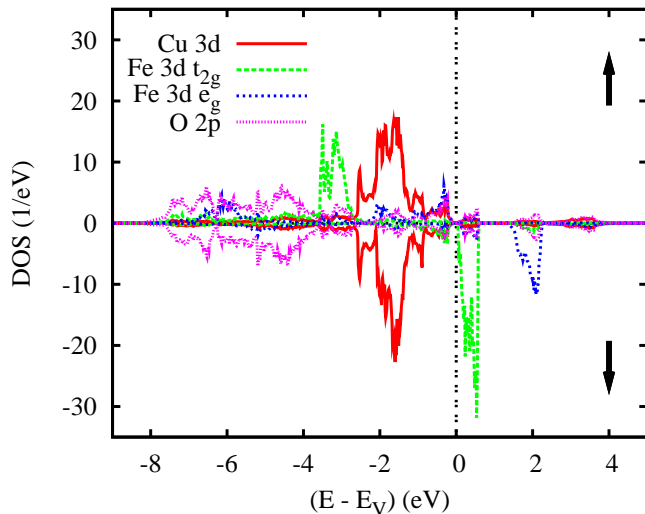


FIG. 3: (Color online) Partial densities of states (DOS) of monoclinic antiferromagnetic high-spin CuFeO_2 .

Thus the non-local exchange interaction included in the GGA leads to the semiconducting ground state once the monoclinic structure is correctly accounted for. However, the band gap is too small reflecting the well known shortcomings of the GGA. Additional inclusion of electronic correlations, for instance via the LDA+U method, is needed to achieve quantitative agreement with experiment.

In summary, our calculations for CuFeO_2 demonstrate that i) taking the monoclinic structure into account results in an antiferromagnetic ground state in perfect agreement with the experimental situation, ii) a fundamental band gap is opened already within the GGA, and iii) there is a quite unusual competition among several magnetic states, including *three* different magnetic states of assumed ferromagnetic CuFeO_2 , which so far seems not to have been obtained for iron compounds. Concerning the latter point it is remarkable that the trigonal environment of Fe^{3+} renders its magnetic states very close in energy, while under most circumstances Fe^{3+} is in the high spin state. Even though the effect is less pronounced than in the calcium cobaltates, where the environment has a dramatic effect on the spin configuration of the Co^{3+} ions [30, 31], this opens a route to the observation of spin state transitions in Fe^{3+} ions as well.

ACKNOWLEDGEMENTS

We gratefully acknowledge many useful discussions with T. Kopp, C. Martin, and W. C. Sheets. This work was supported by the Deutsche Forschungsgemeinschaft through SFB 484.

- * Electronic address: eyert@physik.uni-augsburg.de; Permanent address: Center for Electronic Correlations and Magnetism, Institut für Physik, Universität Augsburg, 86135 Augsburg, Germany
- [1] H. Kageyama, K. Yoshimura, K. Kosuge, H. Mitamura, and T. Goto, *J. Phys. Soc. Japan* **66**, 1607 (1997).
 - [2] A. Maignan, C. Michel, A. C. Masset, C. Martin, and B. Raveau, *Eur. Phys. J. B* **15**, 657 (2000).
 - [3] V. Hardy, C. Martin, G. Martinet, and G. André, *Phys. Rev. B* **74**, 064413 (2006).
 - [4] R. D. Shannon, D. B. Rogers, and C. T. Prewitt, *Inorg. Chem.* **10**, 713 (1971); C. T. Prewitt, R. D. Shannon, and D. B. Rogers, *ibid.* **10**, 719 (1971); D. B. Rogers, R. D. Shannon, C. T. Prewitt, and J. L. Gillson, *ibid.* **10**, 723 (1971).
 - [5] H. Kawazoe, M. Yasukawa, H. Hyodo, M. Kurita, H. Yanagi, and H. Hosono, *Nature* **389**, 939 (1997).
 - [6] V. Eyert, R. Frésard, and A. Maignan, arXiv:0801.4077 (unpublished)
 - [7] A. H. Muir and M. Wiedersich, *J. Phys. Chem. Solids* **28**, 65 (1967).
 - [8] J.-P. Doumerc, A. Wichainchai, A. Ammar, M. Pouchard, and P. Hagenmuller, *Mat. Res. Bull.* **21**, 745 (1986).
 - [9] M. Mekata, N. Yaguchi, T. Takagi, S. Mitsuda, and H. Yoshizawa, *J. Magn. Magn. Mater.* **104-107**, 823 (1992).
 - [10] M. Mekata, N. Yaguchi, T. Takagi, T. Sugino, S. Mitsuda, H. Yoshizawa, N. Hosoito, and T. Shinjo, *J. Phys. Soc. Japan* **62**, 4474 (1993).
 - [11] O. A. Petrenko, G. Balakrishnan, M. R. Lees, D. McK. Paul, and A. Hoser, *Phys. Rev. B* **62**, 8983 (2000).
 - [12] T. Kimura, J. C. Lashley, and A. P. Ramirez, *Phys. Rev. B* **73**, 220401(R) (2006).
 - [13] S. Seki, Y. Yamasaki, Y. Shiomi, S. Iguchi, Y. Onose, and Y. Tokura, *Phys. Rev. B* **75**, 100403(R) (2007).
 - [14] F. Ye, Y. Ren, Q. Huang, J. A. Fernandez-Baca, P. Dai, J. W. Lynn, and T. Kimura, *Phys. Rev. B* **73**, 220404(R) (2006).
 - [15] V. R. Galakhov, A. I. Poteryaev, E. Z. Kurmaev, V. I. Anisimov, S. Bartkowski, M. Neumann, Z. W. Lu, B. M. Klein, and T.-R. Zhao, *Phys. Rev. B* **56**, 4584 (1997);
 - [16] R. Seshadri, C. Felser, K. Thieme, and W. Tremel, *Chem. Mater.* **10**, 2189 (1998);
 - [17] K. P. Ong, K. Bai, P. Blaha, and P. Wu, *Chem. Mater.* **19**, 634 (2007);
 - [18] D. J. Singh, *Phys. Rev. B* **76**, 085110 (2007).
 - [19] V. L. Moruzzi, P. M. Marcus, K. Schwarz, and P. Mohn, *Phys. Rev. B* **34**, 1784 (1986).
 - [20] J. P. Perdew, K. Burke, and M. Ernzerhof, *Phys. Rev. Lett.* **77**, 3865 (1996).
 - [21] J. P. Perdew and Y. Wang, *Phys. Rev. B* **45**, 13244 (1992).
 - [22] A. R. Williams, J. Kübler, and C. D. Gelatt, Jr., *Phys. Rev. B* **19**, 6094 (1979).
 - [23] V. Eyert, *Int. J. Quantum Chem.* **77**, 1007 (2000).
 - [24] V. Eyert, *The Augmented Spherical Wave Method – A Comprehensive Treatment*, Lect. Notes Phys. **719** (Springer, Berlin Heidelberg 2007).
 - [25] V. Eyert and K.-H. Höck, *Phys. Rev. B* **57**, 12727 (1998).
 - [26] V. Eyert, *J. Comp. Phys.* **124**, 271 (1996).
 - [27] P. E. Blöchl, O. Jepsen, and O. K. Andersen, *Phys. Rev.*

- B **49**, 16223 (1994).
- [28] V. Eyert, J. Comp. Chem., in press.
- [29] M. S. Methfessel, Phys. Rev. B **38**, 1537 (1988).
- [30] V. Eyert, C. Laschinger, T. Kopp, and R. Frésard, Chem. Phys. Lett. **385**, 249 (2004).
- [31] S. Aasland, H. Fjellvåg, and B. C. Hauback, Solid State Comm. **101**, (1997) 187.